

## Stereolabile and Configurationally Stable Atropisomers of Hindered Aryl Carbinols

Daniele Casarini\*

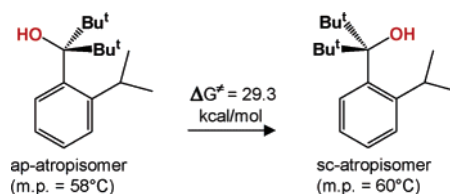
Department of Chemistry, University of Basilicata, Potenza, Italy

Carmine Coluccini,<sup>1</sup> Lodovico Lunazzi, and Andrea Mazzanti\*

Department of Organic Chemistry "A. Mangini", University of Bologna, Viale Risorgimento, 4 Bologna 40136, Italy

mazzand@ms.fci.unibo.it

Received March 1, 2005



Carbinols of the Ar–C(OH)R<sub>2</sub> type, Ar being *o*-isopropylphenyl, exist as stereolabile syn-clinal (*sc*) and anti-periplanar (*ap*) atropisomers when R = Me, Et, *i*-Pr. In the latter compound, the major atropisomer also comprises two enantiomeric forms that interchange with a barrier of 6.4 kcal mol<sup>-1</sup>. X-ray diffraction, NOE experiments, and ab initio calculations indicate that the *sc*-atropisomer is the more stable form when R = Me, *i*-Pr, *t*-Bu but is the less stable one when R = Et. NMR spectra at variable temperature allowed the determination of the barriers for the interconversion of the *sc*- into the *ap*-atropisomers ( $\Delta G^\ddagger = 7.6, 8.8,$  and  $13.5$  kcal mol<sup>-1</sup> for Me, Et, *i*-Pr, respectively). When R is a *tert*-butyl group, the two atropisomers are configurationally stable: the *ap*-atropisomer is obtained as the kinetic controlled compound, which can be transformed into the thermodynamically more stable *sc*-atropisomer with a free energy of activation of 29.3 kcal mol<sup>-1</sup>. Both atropisomers exhibit restricted rotation of the *tert*-butyl moiety, the corresponding  $\Delta G^\ddagger$  values being 9.4 and 8.8 kcal mol<sup>-1</sup> for the *sc*- and *ap*-atropisomer, respectively.

### Introduction

Restricted rotation about the sp<sup>2</sup>–sp<sup>3</sup> bond of Ar–C(OH)R<sub>2</sub> carbinols was detected and the corresponding barrier measured, by variable temperature NMR spectroscopy.<sup>2–9</sup> When the Ar moieties do not possess a 2-fold symmetry axis, two stereolabile atropisomers of different

stability were identified.<sup>3,8</sup> In the case of highly hindered compounds, having as R substituent the *tert*-butyl or the adamantyl moieties, the atropisomers are configurationally stable and can be physically isolated.<sup>5–8</sup>

Here we report the structural, conformational, and stereodynamic properties of a class of carbinols (compounds 1–4 of Chart 1) having substituents of different dimensions, so that either stereolabile or configurationally stable atropisomers can be obtained.

### Results and Discussion

On lowering the temperature, the <sup>1</sup>H and <sup>13</sup>C NMR signals of 1–3 broaden and eventually split into two

(1) In partial fulfillment for a Ph.D. in Chemical Sciences, University of Bologna.

(2) (a) Newsoroff, G. P.; Sternhell, S. *Tetrahedron Lett.* **1967**, 2539. (b) Baas, J. M. A.; Sinnema, A. *Recl. Trav. Chim. Pays-Bas* **1973**, *92*, 899. (c) Baas, J. M. A.; van der Toorn, J. M.; Wepster, B. M. *Recl. Trav. Chim. Pays-Bas* **1974**, *93*, 173.

(3) (a) Landman, D.; Newsoroff, G. P.; Sternhell, S. *Aust. J. Chem.* **1972**, *25*, 109. (b) Suezawa, H.; Wada, H.; Watanabe, H.; Yuzuri, T.; Sakakibara, K.; Hirota, M. *J. Phys. Org. Chem.* **1997**, *10*, 925.

(4) Anderson, S.; Drakenberg, T. *Org. Magn. Reson.* **1983**, *21*, 730.

(5) (a) Lomas, J. S.; Dubois, J.-E. *J. Org. Chem.* **1976**, *41*, 3033. (b) Lomas, J. S.; Luong, P. K.; Dubois, J.-E. *J. Org. Chem.* **1977**, *42*, 3394.

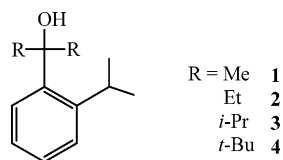
(6) Lomas, J. S.; Dubois, J.-E. *Tetrahedron* **1981**, *37*, 2273. Lomas, J. S.; Vaissermsnn, J. *J. Chem. Soc., Perkin Trans. 2* **1998**, 1777. Lomas, J. S. *J. Chem. Soc., Perkin Trans. 2* **2001**, 754. Lomas, J. S.; Adenier, A. *J. Chem. Soc., Perkin Trans. 2* **2002**, 1264.

(7) (a) Anderson, J. E.; Bru-Capdeville, V.; Kirsch, P. A.: Lomas, J. S. *Chem. Commun.* **1994**, 1077. (b) Lomas, J. S.; Anderson, J. E. *J. Org. Chem.* **1995**, *60*, 3246.

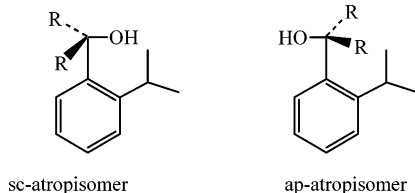
(8) Casarini, D.; Lunazzi, L.; Mazzanti, A. *J. Org. Chem.* **1997**, *62*, 3315.

(9) Wolf, C.; Pranatharthiaran, L.; Ramagosa, R. B. *Tetrahedron* **2002**, *43*, 8567.

## CHART 1



## SCHEME 1



groups of signals of different intensity, indicating the existence of two conformational isomers (stereolabile atropisomers as in Scheme 1). As an example of this behavior, let us examine the  $^{13}\text{C}$  lines due to the two quaternary aromatic carbons of **1** ( $\text{R} = \text{Me}$ ) as displayed in Figure 1. From ambient temperature to  $-50\text{ }^\circ\text{C}$  these two lines are still sharp, but broaden considerably in the  $-90^\circ$  to  $-120\text{ }^\circ\text{C}$  range and split below  $-130\text{ }^\circ\text{C}$ , yielding two pairs of lines, the intensity ratio within each pair being 77:23. The two spectra correspond to the anti-periplanar (ap) and syn-clinal (sc) atropisomers of Scheme 1 ( $\text{R} = \text{Me}$ ).

A complete conformational search was carried out by molecular mechanics (MM) calculations:<sup>10</sup> on each of the two atropisomer structures: the ground-state energy for the sc-atropisomer of **1** is computed to be lower than that for the ap-atropisomer by  $1.9\text{ kcal mol}^{-1}$ . Ab initio calculations<sup>11</sup> confirm that these structures are real energy minima because of the absence of imaginary frequencies in the vibrational analysis. These calculations too predict that the sc-atropisomer has an energy  $1.85\text{ kcal mol}^{-1}$  lower than that of its ap-counterpart (Figure 2), and for this reason the sc structure was tentatively assigned to the more stable of the two atropisomers in solution.<sup>12</sup> Support of this conclusion is offered by the

(10) MMFF force field, as implemented in Titan 1.0.5, Wavefunction Inc., Irvine, CA. A Monte Carlo algorithm (version 1.0.3) was used for locating the global minima.

(11) Frisch, M. J.; Trucks, G. W.; Schlegel, H. B.; Scuseria, G. E.; Robb, M. A.; Cheeseman, J. R.; Montgomery, J. A., Jr.; Vreven, T.; Kudin, K. N.; Burant, J. C.; Millam, J. M.; Iyengar, S. S.; Tomasi, J.; Barone, V.; Mennucci, B.; Cossi, M.; Scalmani, G.; Rega, N.; Petersson, G. A.; Nakatsuji, H.; Hada, M.; Ehara, M.; Toyota, K.; Fukuda, R.; Hasegawa, J.; Ishida, M.; Nakajima, T.; Honda, Y.; Kitao, O.; Nakai, H.; Klene, M.; Li, X.; Knox, J. E.; Hratchian, H. P.; Cross, J. B.; Bakken, V.; Adamo, C.; Jaramillo, J.; Gomperts, R.; Stratmann, R. E.; Yazyev, O.; Austin, A. J.; Cammi, R.; Pomelli, C.; Ochterski, J. W.; Ayala, P. Y.; Morokuma, K.; Voth, G. A.; Salvador, P.; Dannenberg, J. J.; Zakrzewski, V. G.; Dapprich, S.; Daniels, A. D.; Strain, M. C.; Farkas, O.; Malick, D. K.; Rabuck, A. D.; Raghavachari, K.; Foresman, J. B.; Ortiz, J. V.; Cui, Q.; Baboul, A. G.; Clifford, S.; Cioslowski, J.; Stefanov, B. B.; Liu, G.; Liashenko, A.; Piskorz, P.; Komaromi, I.; Martin, R. L.; Fox, D. J.; Keith, T.; Al-Laham, M. A.; Peng, C. Y.; Nanayakkara, A.; Challacombe, M.; Gill, P. M. W.; Johnson, B.; Chen, W.; Wong, M. W.; Gonzalez, C.; Pople, J. A. *Gaussian 03*, Revision C.02; Gaussian, Inc.: Wallingford, CT, 2004.

(12) According to the calculated energy difference between the two atropisomers of **1** (and of **3** as well), the population of the minor form should be negligible: the agreement with the NMR experiment is therefore only qualitative. On the other hand, the computed energy difference in the case of **2** and **4** (Table 1) matches the NMR experiment, since the populations of the minor forms are predicted to be  $\approx 30\%$  and  $0\%$ , respectively, as observed.

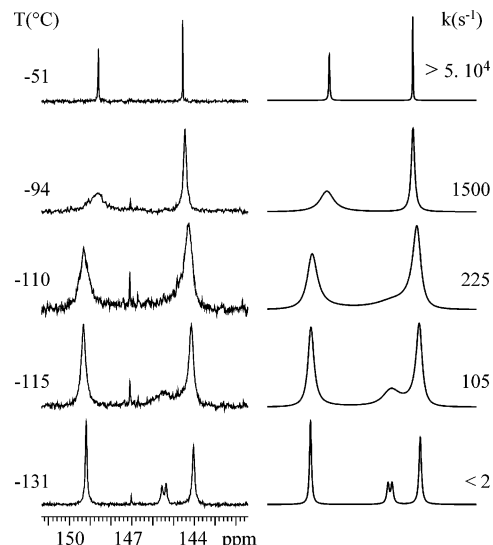


**FIGURE 1.** (Left) Temperature dependence of the  $^{13}\text{C}$  NMR signals (150.8 MHz in  $\text{CHF}_2\text{Cl}/\text{CHFCl}_2$ ) of the two aromatic quaternary carbons of compound **1** ( $\text{R} = \text{Me}$ ). (Right) Simulation obtained with the rate constants indicated.

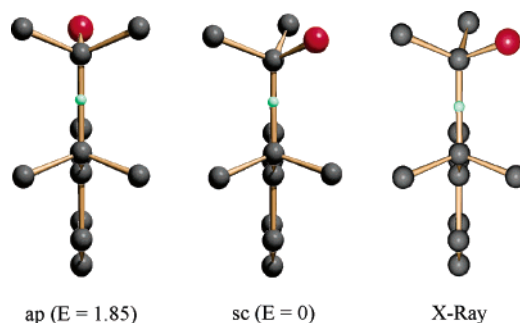


**FIGURE 2.** Ab initio computed structures of the ap- and sc-atropisomers of **1** (the energy values  $E$  are in  $\text{kcal mol}^{-1}$ ). The experimental structure of the sc-atropisomer, obtained by X-ray diffraction, is also reported. With the exception of the CH hydrogen of the *o*-isopropyl substituent (green), the hydrogen atoms are omitted for convenience.

X-ray diffraction of **1**, which shows how the structure determined in the crystalline state corresponds to that of the sc-atropisomer (Figure 2).

According to calculations, the minor ap-atropisomer has a molecular plane of symmetry coincident with that of the phenyl ring (Figure 2, left), thus accounting for the observed equivalence at any temperature of the  $^1\text{H}$  and  $^{13}\text{C}$  NMR signals due to the enantiotopic methyl groups bonded to the C–OH moiety. On the contrary, the major sc-atropisomer (Figure 2, center and right) has the O–C–C1 plane (C1 being the phenyl carbon ortho to the isopropyl substituent) twisted with respect to that of the phenyl ring, the corresponding dihedral angle being  $44^\circ$  (MM),  $46^\circ$  (ab initio), or  $52.2^\circ$  (X-ray). Such a structure is therefore asymmetric, thus chiral, and indeed the 16 molecules comprised in the crystal cell (Supporting Information) have opposite M and P configurations (eight molecules for each configuration). The methyl groups bonded to the C–OH moiety are therefore diastereotopic in the solids, yet they yield a single line in the NMR solution spectrum, even at  $-150\text{ }^\circ\text{C}$ . This indicates that the interconversion of the two M and P enantiomers of

**TABLE 1.** Interconversion Barriers ( $\Delta G^\ddagger$  in kcal mol<sup>-1</sup>), Atropisomer Ratio, and Ab Initio Computed Energy Difference (kcal mol<sup>-1</sup>) for Compounds 1–4

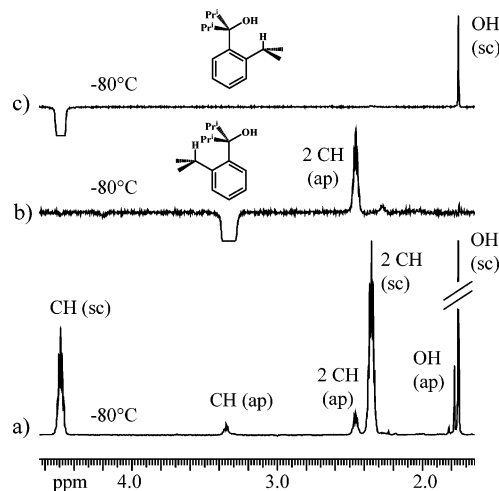
compd (R)	sc/ap ratio	solvent	$\Delta G^\ddagger$		$E_{ap} - E_{sc}$
			sc to ap	ap to sc	
1 (Me)	77/23 (at -131 °C)	CHF <sub>2</sub> Cl/CHFCl <sub>2</sub>	7.6	7.3 <sub>5</sub>	1.85
2 (Et)	35/65 (at -115 °C)	CHF <sub>2</sub> Cl	8.8	9.0	-0.3
3 ( <i>i</i> -Pr)	88/12 (at -45 °C)	CHF <sub>2</sub> Cl/CHFCl <sub>2</sub>	13.5	12.6	2.2
4 ( <i>t</i> -Bu)	100/0 (at 100 °C)	C <sub>2</sub> Cl <sub>4</sub>	–	29.3	6.75

the sc-atropisomer is very rapid in solution in that the passage of the OH group across the *o*-isopropyl substituent involves a rather low barrier. The corresponding computed value is indeed too small (3.2 or 3.6 kcal mol<sup>-1</sup> according to MM or ab initio calculations, respectively) to allow detection of different NMR signals for the mentioned methyl groups at any attainable temperature. In other words, such a fast motion generates, in practice, a dynamic plane of symmetry that makes these methyl groups appear equivalent (enantiotopic) in solution.

The interconversion rates of the more into the less stable atropisomer of **1** were determined by line shape simulation at different temperatures, as shown in Figure 1: the corresponding free energy of activation<sup>13</sup> could thus be obtained ( $\Delta G^\ddagger = 7.6 \pm 0.15$  kcal mol<sup>-1</sup>, as in Table 1). Such a process requires the passage of one methyl group across the *o*-isopropyl substituent: the energy calculated for this transition state with respect to the sc ground state of **1** (7.0 and 7.1 kcal mol<sup>-1</sup> in the MM and ab initio computations, respectively) is in good agreement with the experiment.

Analogous results were obtained for derivatives **2** (R = Et) and **3** (R = *i*-Pr), where the interconversion barriers were found to increase regularly because of the larger steric requirements: the corresponding interconversion barriers and atropisomer ratios are collected in Table 1. It should be pointed out that in the case of **2** (R = Et) the ratio is reversed, in that to the major atropisomer the ap structure has been assigned. To understand on which ground an opposite stability was attributed to the atropisomers of **2**, it is necessary to illustrate how the experimental assignment was achieved in the case of compounds **3** and **4**.

Unambiguous assignment of the structure of the two atropisomers could be obtained in the case of **3** (R = *i*-Pr) by making use of NOE experiments carried out at -80 °C. On the basis of the measured barrier of **3**, it is in

**FIGURE 3.** NOE experiments (600 MHz at -80 °C in CD<sub>2</sub>Cl<sub>2</sub>) carried out by excitation of the CH multiplet of the *o*-isopropyl group of the minor and major atropisomer of compound **3** (traces b and c, respectively). The control spectrum in the region 1.6–4.6 ppm (trace a) is also reported.

fact expected that these atropisomers are sufficiently long living at -80 °C to prevent the occurrence of saturation transfer effects.<sup>14</sup> Excitation of the CH multiplet of the *o*-isopropyl substituent in the major atropisomer enhances the corresponding OH line (trace c of Figure 3). Excitation of the same hydrogen signal in the minor atropisomer enhances the corresponding CH multiplet of the two isopropyl groups bonded to C–OH (trace b of Figure 3). This means that for the major atropisomer the structure must be of the sc type and in the minor of the ap type.

As a consequence of the proximity of the OH group, the shift of the CH multiplet of the *o*-isopropyl substituent of **3** is at lower field in the major sc-atropisomer (4.45 ppm) than in the minor ap-atropisomer (3.38 ppm). The same trend had been also observed in the case of **1** (R = Me), where the assignment of the sc-atropisomer relied on the X-ray diffraction data (the corresponding *o*-isopropyl CH hydrogen has the shift of the sc-atropisomer at 4.7 and that of the ap-atropisomer at 3.8 ppm). Again in the case of **4** (see further), the unambiguously assigned (NOE experiments<sup>15,16</sup>) sc-atropisomer has the signal of the mentioned CH hydrogen downfield (4.56 ppm) with respect to that of the ap-atropisomer (3.54 ppm). The trend of these shifts can thus be used as a criterion for

(13) In the restricted temperature range where this dynamic process could be monitored, the free energy of activation was found to be essentially constant within the experimental errors, suggesting a negligible value for the activation entropy, as often observed in conformational processes. See: Hoogosian, S.; Bushweller, C. H.; Anderson, W. G.; Kigsley, G. *J. Phys. Chem.* **1976**, *80*, 643. Lunazzi, L.; Cerioni, G.; Ingold, K. U. *J. Am. Chem. Soc.* **1976**, *98*, 7484. Bernardi, F.; Lunazzi, L.; Zanirato, P.; Cerioni, G. *Tetrahedron* **1977**, *33*, 1337. Lunazzi, L.; Magagnoli, C.; Guerra, M.; Macciantelli, D. *Tetrahedron Lett.* **1979**, 3031. Cremonini, M. A.; Lunazzi, L.; Placucci, G.; Okazaki, R.; Yamamoto, G. *J. Am. Chem. Soc.* **1990**, *112*, 2915. Anderson, J. E.; Tocher, D. A.; Casarini, D.; Lunazzi, L. *J. Org. Chem.* **1991**, *56*, 1731. Borghi, R.; Lunazzi, L.; Placucci, G.; Cerioni, G.; Foresti, E.; Plumitalo, A. *J. Org. Chem.* **1997**, *62*, 4924. Garcia, M. B.; Grilli, S.; Lunazzi, L.; Mazzanti, A.; Orelli, L. R. *J. Org. Chem.* **2001**, *66*, 6679. Garcia, M. B.; Grilli, S.; Lunazzi, L.; Mazzanti, A.; Orelli, L. R. *Eur. J. Org. Chem.* **2002**, 4018. Casarini, D.; Rosini, C.; Grilli, S.; Lunazzi, L.; Mazzanti, A. *J. Org. Chem.* **2003**, *68*, 1815. Casarini, D.; Grilli, S.; Lunazzi, L.; Mazzanti, A. *J. Org. Chem.* **2004**, *69*, 345. Bartoli, G.; Lunazzi, L.; Massacesi, M.; Mazzanti, A. *J. Org. Chem.* **2004**, *69*, 821. Casarini, D.; Coluccini, C.; Lunazzi, L.; Mazzanti, A.; Rompietti, R. *J. Org. Chem.* **2004**, *69*, 5746.

(14) At -50 °C there is still a saturation transfer effect, since irradiation of the *o*-isopropyl CH signal of the major atropisomer affects also the corresponding signal of the minor atropisomer and vice versa. On the contrary, at -80 °C this effect had disappeared, as clearly evident from Figure 3, where saturation of the major CH signal leaves unaffected the minor one (trace c) and likewise saturation of the minor leaves the major signal unaffected (trace b).

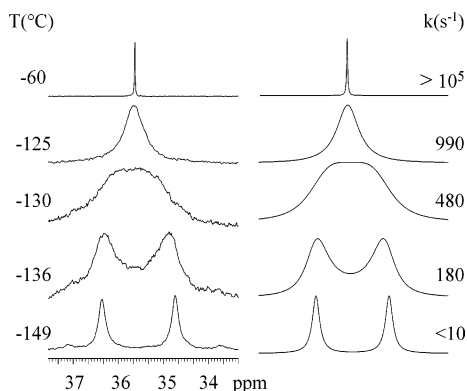


**FIGURE 4.** (Left) Temperature dependence of the  $^{13}\text{C}$  NMR (150.8 MHz in  $\text{CHF}_2\text{Cl}/\text{CHFCl}_2$ ) signals of the methine carbons of the two isopropyl groups bonded to the C–OH moiety of **3**. (Right) Simulation obtained with the rate constants indicated.

identifying the atropisomers: in the case of **2**, the major (65%) signal of the *o*-isopropyl CH multiplet is, on the contrary, upfield (3.3 ppm) with respect to the minor one (4.2 ppm), indicating that the more stable atropisomer of **2** has the ap structure. Furthermore, the same ab initio computations that had indicated the sc-atropisomer to be the more stable form in **1**, **3**, and **4** predict that the ap-atropisomer has an energy lower by 0.3 kcal mol $^{-1}$  than that of the sc-atropisomer of **2** (Table 1). What causes the inversion of the stability of the atropisomers of **2** with respect to those of **1**, **3**, and **4** is still unclear.

The major sc-atropisomer of **3** undergoes a second dynamic process, which was detected by cooling the sample at even lower temperatures. The  $^{13}\text{C}$  signals of the  $\text{CH}_3$  and CH carbons of the two isopropyl groups bonded to the C–OH moiety broaden and eventually split, displaying four lines of equal intensity for the methyl and two lines of equal intensity for the methine carbons at  $-149$  °C (Figure 4). This proves that the rotation of the two isopropyl groups has been frozen and, in addition, that the molecule has adopted an asymmetric, thus chiral, conformation. Ab initio calculations<sup>11</sup> confirm that the global energy minimum for the sc-atropisomer of **3** corresponds to a structure where the C–H bonds of the two isopropyl groups point into opposite directions (Figure 5), thus making all six corresponding carbons diastereotopic. The temperature dependence of the  $^{13}\text{C}$  signals of the two isopropyl CH carbons is displayed in Figure 4, and from the measured rate constants the barrier for the interconversion of the two enantiomers of Figure 5, brought about by the rotation of the isopropyl groups, was determined ( $\Delta G^\ddagger = 6.4 \pm 0.15$  kcal mol $^{-1}$ ).<sup>13</sup>

(15) Excitation of the *tert*-butyl line enhances, in addition to the OH line, the methine and methyl signals of the *o*-isopropyl substituent, and likewise, excitation of the methine signal of the latter substituent enhances the line of the *tert*-butyl groups but not that of the OH. On the other hand, excitation of the OH line enhances the *tert*-butyl line and also one CH aromatic signal, but does not have any effect on the signals of the *o*-isopropyl substituent. This proves that the OH group is directed away from the *o*-isopropyl substituent (hence ap-atropisomer).

(16) Excitation of the OH line enhances, in addition to the *tert*-butyl line, both the methine and methyl signals of the *o*-isopropyl substituent (but does not have any effect on any aromatic hydrogen signals), and likewise, excitation of the CH multiplet enhances the OH line. This indicates that the OH group is directed toward the *o*-isopropyl substituent (hence the sc-atropisomer).

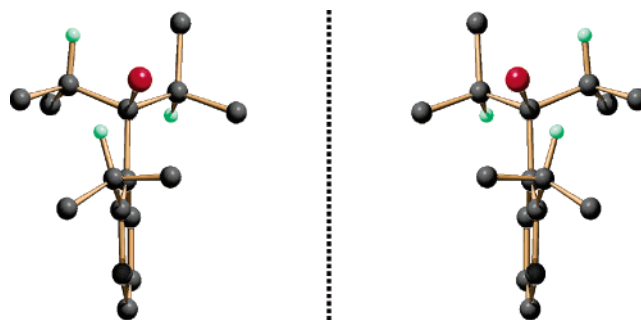


**FIGURE 5.** Ab initio computed structures of the two enantiomeric forms of the sc-atropisomer of compound **3**. With the exception of the CH hydrogen of the three isopropyl substituents (green), the hydrogen atoms are omitted for convenience.

Compound **4**, which bears two *tert*-butyl substituents, is hindered enough as to yield, in principle, two configurationally stable atropisomers. The reaction (see Experimental Section) produced, however, only one atropisomer (indicated as **4b**), to which the ap configuration was unambiguously assigned by means of NOE experiments (Supporting Information).<sup>15</sup> When a tetrachloroethylene solution of **4b** is kept overnight at 100 °C, a complete interconversion into the sc-atropisomer **4a** was obtained (the sc-configuration was also confirmed by means of NOE experiments<sup>16</sup>). This indicates that the latter is the thermodynamically more stable atropisomer, whereas the ap-atropisomer **4b** is the result of a kinetic preference.

The transformation rate of the ap- into the sc-atropisomer (i.e. **4b** into **4a**) was followed at 100 °C by monitoring the time-dependent variation of the relative intensities of the NMR spectra in  $\text{C}_2\text{Cl}_4$ . From the rate constant obtained in this way ( $k = 5 \times 10^{-5}$  s $^{-1}$ ) a  $\Delta G^\ddagger$  value of 29.3 kcal mol $^{-1}$  (Table 1) was derived.

Both the sc- (**4a**) and ap-atropisomers (**4b**) exhibit restricted rotation of the *tert*-butyl groups. For example, the single  $^{13}\text{C}$  line of the methyl carbons broadens on cooling and finally splits into three equally intense signals below  $-130$  °C (Supporting Information). The rotational barriers derived by line shape simulation are slightly different, being 9.4 and 8.8 kcal mol $^{-1}$  for **4a** and **4b**, respectively.

As is plausible, MM and ab initio calculations predict that one *tert*-butyl group is not eclipsed but staggered with respect to the other; in other words, the three Me–C bonds of one *tert*-butyl group are rotated by 30° with respect to those of the other. When the rotation is frozen, such an arrangement would yield six  $^{13}\text{C}$  methyl lines (and two quaternary carbon lines as well) for each atropisomer, contrary to the experimental evidence. To account for the experimental observation, a fast oscillatory motion (libration process) that exchanges the reciprocal positions of the two *tert*-butyl methyl groups must take place. It is reasonable to expect that the barrier for such a motion is much lower than that for the rotation required to exchange the three methyl groups *within* each of the two *tert*-butyl moieties, and thus is NMR invisible. Indeed MM calculations confirm that the barriers for this libration process are as low as 3.9 and 3.5 kcal mol $^{-1}$  for the sc- and ap-atropisomers, respectively.

## Experimental Section

**Materials. 2-(2-Isopropylphenyl)propan-2-ol (1).**<sup>17</sup> 1-Bromo-2-isopropylbenzene (5 mmol in 15 mL of dry THF) was added to a suspension of Mg (5 mmol) and I<sub>2</sub> in 15 mL of dry THF. After warming for 30 min, the solution was stirred for additional 60 min at room temperature and then treated with propan-2-one (5 mmol in 15 mL of dry THF). After stirring for 3 h, the mixture was treated with H<sub>2</sub>O, extracted with ether, and dried (Na<sub>2</sub>SO<sub>4</sub>). After removing the solvent, the crude product was purified by a silica gel chromatography column (petroleum ether/Et<sub>2</sub>O 9/1) to give **1** (2.9 mmol, overall yield 58%). Crystals suitable for X-ray diffraction were obtained from absolute ethanol: mp 65 °C; <sup>1</sup>H NMR (CDCl<sub>3</sub>, 400 MHz) δ 1.25 (6H, d, *J* = 6.9 Hz), 1.68 (6H, s), 1.75 (1H, s, OH), 3.88 (1H, eptet, *J* = 6.9 Hz), 7.10 (1H, m), 7.26 (1H, m), 7.38 (1H, m), 7.42 (1H, m); <sup>13</sup>C NMR (CDCl<sub>3</sub>, 100.6 MHz) δ 24.7 (2CH<sub>3</sub>), 29.2 (CH), 31.6 (CH<sub>3</sub>), 73.5 (Cq), 124.8 (CH), 125.2 (CH), 127.3 (CH), 127.7 (CH), 144.2 (Cq), 148.0 (Cq). Anal. Calcd for C<sub>12</sub>H<sub>18</sub>O: C, 80.85; H, 10.18. Found. C, 80.05; H, 10.07.

**3-(2-Isopropylphenyl)pentan-3-ol (2).** BuLi (3.1 mL, 1.6 M) in hexane was added to solution of 1-bromo-2-isopropylbenzene (5 mmol in 15 mL of dry THF) at -78 °C. The solution was stirred for 60 min and then treated with pentan-3-one (5 mmol in 15 mL of dry THF). After stirring for 10 min, the mixture was warmed to 25 °C and treated with H<sub>2</sub>O, extracted with ether, and dried (Na<sub>2</sub>SO<sub>4</sub>). After removing the solvent, the crude was purified by a silica gel chromatography column (petroleum ether/Et<sub>2</sub>O 19/1) to give **2** (2.5 mmol, overall yield 50%): <sup>1</sup>H NMR (CDCl<sub>3</sub>, 300 MHz) δ 0.78 (6H, t), 1.21 (6H, d, *J* = 6.9 Hz), 1.89 (2H, m), 2.01 (2H, m), 3.67 (1H, eptet, *J* = 6.9 Hz), 7.14 (1H, m), 7.22 (1H, m), 7.33 (1H, m), 7.42 (1H, m); <sup>13</sup>C NMR (CDCl<sub>3</sub>, 75.4 MHz) δ 8.3 (CH<sub>3</sub>), 22.5 (Cq), 24.7 (CH<sub>3</sub>), 29.4 (CH<sub>2</sub>), 33.9 (CH<sub>3</sub>), 78.5 (Cq), 125.0 (CH), 126.9 (CH), 127.0 (CH), 127.4 (CH), 141.2 (Cq), 147.0 (Cq). Anal. Calcd for C<sub>14</sub>H<sub>22</sub>O: C, 81.50; H, 10.75. Found. C, 80.67; H, 10.63.

**3-(2-Isopropylphenyl)-2,4-dimethylpentan-3-ol (3).** BuLi (3.1 mL, 1.6 M) in hexane was added to solution of 1-bromo-2-isopropylbenzene (5 mmol in 15 mL of dry THF) at -78 °C. The solution was stirred for 60 min and treated with 2,4-dimethylpentan-3-one (5 mmol in 15 mL of dry THF). After stirring for 10 min, the mixture was warmed to 25 °C, treated with H<sub>2</sub>O, extracted with ether, and dried (Na<sub>2</sub>SO<sub>4</sub>). After removing the solvent, the crude was purified by a silica gel chromatography column (petroleum ether/Et<sub>2</sub>O 9/1) to give **3** (1.9 mmol, overall yield 38%): <sup>1</sup>H NMR (CDCl<sub>3</sub>, 600 MHz) δ 0.78 (6H, bd), 0.94 (6H, bd), 1.21 (6H, d, *J* = 6.8 Hz), 1.59 (1H, s, OH), 2.38 (2H, bs), 4.48 (1H, bs), 7.07 (2H, bs), 7.18 (1H, bt), 7.37 (1H, bd); <sup>13</sup>C NMR (CDCl<sub>3</sub>, 150.8 MHz) δ 16.8 (CH), 17.9 (CH), 25.3 (2 CH<sub>3</sub>), 29.2 (CH), 35.5 (CH<sub>3</sub>), 85.2 (Cq), 124.0 (CH), 126.3 (CH), 127.4 (CH), 127.9 (CH), 138.2 (Cq), 150.6 (Cq). Anal. Calcd for C<sub>16</sub>H<sub>26</sub>O: C, 81.99; H, 11.18. Found C, 81.16; H, 11.07.

**3-(2-Isopropylphenyl)-2,2,4,4-tetramethylpentan-3-ol (4b), ap-Atropisomer.** *t*-BuLi (3.1 mL, 1.5 M) in pentane was added to a solution of 1-bromo-2-isopropylbenzene (5 mmol in 15 mL of dry THF) at -78 °C. The solution was stirred for 60 min and then treated with 2,2,4,4-tetramethylpentan-3-one (5 mmol in 15 mL of dry THF). After stirring for 10 min, the mixture was warmed to 25 °C, treated with H<sub>2</sub>O, extracted with ether, and dried (Na<sub>2</sub>SO<sub>4</sub>). After removing the solvent, the crude was purified by a silica gel chromatography column (petroleum ether/Et<sub>2</sub>O 9/1) to give **4b** (2.2 mmol, overall yield 44%): mp 58 °C; <sup>1</sup>H NMR (CDCl<sub>3</sub>, 600 MHz) δ 1.15 (18H, s, *t*-Bu), 1.30 (6H, d, *J* = 6.7 Hz), 1.98 (1H, s, OH), 3.54 (1H, eptet, *J* = 6.7 Hz), 7.13 (1H, m), 7.21 (1H, m), 7.37 (1H, m),

8.03 (1H, m); <sup>13</sup>C NMR (CDCl<sub>3</sub>, 150.8 MHz) δ 26.0 (CH<sub>3</sub>), 30.3 (CH<sub>3</sub>), 31.4 (CH), 42.6 (Cq), 87.4 (Cq), 125.1 (CH), 126.5 (CH), 127.7 (CH), 129.8 (CH), 144.4 (Cq), 146.8 (Cq). Anal. Calcd for C<sub>18</sub>H<sub>30</sub>O: C, 82.38; H, 11.52. Found C, 82.03; H, 11.45.

**3-(2-Isopropylphenyl)-2,2,4,4-tetramethylpentan-3-ol (4a), sc-Atropisomer.** A tetrachloroethylene solution of **4b** was kept overnight at 100 °C to yield quantitatively the *sc*-atropisomer **4a**: mp 60 °C; <sup>1</sup>H NMR (CDCl<sub>3</sub>, 600 MHz) δ 1.14 (18H, s, *t*-Bu), 1.20 (6H, d, *J* = 6.9 Hz), 1.97 (1H, s, OH), 4.56 (1H, eptet, *J* = 6.9), 6.99 (1H, m), 7.16 (1H, m), 7.35 (1H, m), 7.47 (1H, m); <sup>13</sup>C NMR (CDCl<sub>3</sub>, 150.8 MHz) δ 25.2 (CH<sub>3</sub>), 29.2 (CH), 30.0 (CH<sub>3</sub>), 43.4 (2Cq), 88.6 (Cq), 122.2 (CH), 125.9 (CH), 127.6 (CH), 129.8 (CH), 141.3 (Cq), 149.6 (Cq). Anal. Calcd for C<sub>18</sub>H<sub>30</sub>O: C, 82.38; H, 11.52. Found C, 82.17; H, 11.41.

**NMR Measurements.** NMR spectra were recorded at 300, 400, or 600 MHz for <sup>1</sup>H and 75.4, 100.6, or 150.8 MHz for <sup>13</sup>C. The assignments of the <sup>13</sup>C signals were obtained by DEPT and 2D experiments (gHSQC sequence). The NOE experiments were obtained by means of the DPGFSE-NOE sequence<sup>18</sup> using a "rsnob" selective pulse (typically 37 ms) and a mixing time of 2.0 s at ambient temperature or 0.8 s at -80 °C. The samples for the <sup>13</sup>C NMR low-temperature measurements were prepared by connecting to a vacuum line the NMR tubes containing the compound and some C<sub>6</sub>D<sub>6</sub> for locking purpose and condensing therein the gaseous CHF<sub>3</sub>Cl and CHFCl<sub>2</sub> under cooling with liquid nitrogen. The tubes were subsequently sealed in vacuo and introduced into the precooled probe of the spectrometer. The temperatures were calibrated by substituting the sample with a precision Cu/Ni thermocouple before the measurements. Complete fitting of dynamic NMR line shapes was carried out using a PC version of the DNMR-6 program.<sup>19</sup> At least five different temperature spectra were used for the simulations.

**Computations.** A complete conformational search, using molecular mechanics (MMFF force field<sup>10</sup>), was performed to locate the global minima of the two atropisomers of **1-4**; ab initio computations were carried out on these structures at the B3LYP/6-31G(d) level by means of the Gaussian 03 series of programs<sup>11</sup> (the standard Berny algorithm in redundant internal and default criteria of convergence were employed). Harmonic vibrational frequency were calculated in order to ascertain the nature of all the stationary points. For each optimized ground state the frequency analysis showed the absence of imaginary frequencies, whereas for each transition state the frequency analysis showed a single imaginary frequency. The corresponding optimized structures are reported in the Supporting Information.

**Acknowledgment.** Financial support from the University of Bologna (Funds for selected research topics and RFO) and from MIUR-COFIN 2003, Rome (national project "Stereoselection in Organic Synthesis") was received by L.L. and A.M.

**Supporting Information Available:** Crystal data for compound **1**, temperature dependence of the <sup>13</sup>C NMR spectra and NOE experiments for **4a** and **4b**, and computational data for compounds **1-4**. This material is available free of charge via the Internet at <http://pubs.acs.org>.

JO050382X

(17) Brown, H. C.; Brady, J. D.; Grayson, M.; Bonner, W. H. *J. Am. Chem. Soc.* **1957**, *79*, 1897.

(18) (a) Stott, K.; Stonehouse, J.; Keeler, J.; Hwand, T.-L.; Shaka, A. J. *J. Am. Chem. Soc.* **1995**, *117*, 4199. (b) Stott, K.; Keeler, J.; Van, Q. N.; Shaka, A. J. *J. Magn. Reson.* **1997**, *125*, 302. (c) Van, Q. N.; Smith, E. M.; Shaka, A. J. *J. Magn. Reson.* **1999**, *141*, 191. (d) See also: Claridge, T. D. W. *High-Resolution NMR Techniques in Organic Chemistry*; Pergamon: Amsterdam, 1999.

(19) PC version of the QCPE program no. 633, Indiana University, Bloomington, IN.